Chemical Science

EDGE ARTICLE

View Article Online
View Journal | View Issue

CrossMark click for updates

Cite this: *Chem. Sci.*, 2015, **6**, 4730

Fe(IV) alkylidenes *via* protonation of Fe(II) vinyl chelates and a comparative Mössbauer spectroscopic study†

Brian M. Lindley,[a] Ala'aeddeen Swidan,[a] Emil B. Lobkovsky,[a] Peter T. Wolczanski,*[a] Mario Adelhardt,[b] Jörg Sutter[b] and Karsten Meyer[b]

Received 8th April 2015
Accepted 20th May 2015

DOI: 10.1039/c5sc01268f

www.rsc.org/chemicalscience

Treatment of *cis*-$Me_2Fe(PMe_3)_4$ with di-1,2-(*E*-2-(pyridin-2-yl)vinyl)benzene ($(bdvp)H_2$), a tetradentate ligand precursor, afforded $(bdvp)Fe(PMe_3)_2$ (**1**-PMe_3) and 2 equiv. CH_4, *via* C–H bond activation. Similar treatments with tridentate ligand precursors $PhCH{=}NCH_2(E\text{-}CH{=}CHPh)$ ($(pipp)H_2$) and $PhCH{=}N(2\text{-}CCMe\text{-}Ph)$ ((pipa)H) under dinitrogen provided *trans*-$(pipp)Fe(PMe_3)_2N_2$ (**2**) and *trans*-(pipvd)$Fe(PMe_3)_2N_2$ (**3**), respectively; the latter *via* one C–H bond activation, and a subsequent insertion of the alkyne into the remaining Fe–Me bond. All three Fe(II) vinyl species were protonated with $H[BAr^F{}_4]$ to form the corresponding Fe(IV) alkylidene cations, $[(bavp)Fe(PMe_3)_2][BAr^F{}_4]$ (**4**-PMe_3), $[(piap)Fe(PMe_3)_3][BAr^F{}_4]$ (**5**), and $[(pipad)Fe(PMe_3)_3][BAr^F{}_4]$ (**6**). Mössbauer spectroscopic measurements on the formally Fe(II) and Fe(IV) derivatives revealed isomer shifts within 0.1 mm s^{-1}, reflecting the similarity in their bond distances.

Introduction

Homogeneous alkylidene compounds that catalyze olefin metathesis[1–5] typically contain 2nd row transition metals that have modest limitations regarding functionality tolerance (*e.g.*, Mo),[1,2] and relative abundance (*e.g.*, Ru).[3,4] Applications for commodity chemicals production have been hampered by these factors, and inexpensive first row transition metal alternatives hold great promise for solving some of the problems. Thus far, the synthesis of 1st row transition metal alkylidene complexes has presented a significant challenge to the organometallic community, especially in the case of iron.

Electronic structure analysis by Hoffmann *et al.*[6] suggests that metathesis catalysts need to be d^n ($n \leq 4$), hence Fe(IV) alkylidenes are the target of interest, especially in analogy to their 2nd row congeners. Several Fe(IV) alkylidenes have been synthesized, with two routes utilized in the cases of those structurally characterized (Fig. 1): (1) conversion of $[CpLL'Fe{=}C(OR)R']^+$ *via* hydride or alkyl anion reagents,[7–9] and (2) the addition of diazoalkanes, typically Ph_2CN_2, to coordinatively unsaturated complexes or labile precursors.[10–13] The subsequent chemistry has been limited to carbene transfers, and some transformations that hint at radical reactions.

In an effort to expand the scope of Fe(IV) alkylidenes, and to develop new synthetic paths, Fe(II) vinyl chelates have been explored as potential precursors to cationic Fe(IV) alkylidenes *via* protonation.[14–18] Entry into ferrous vinyl derivatives was

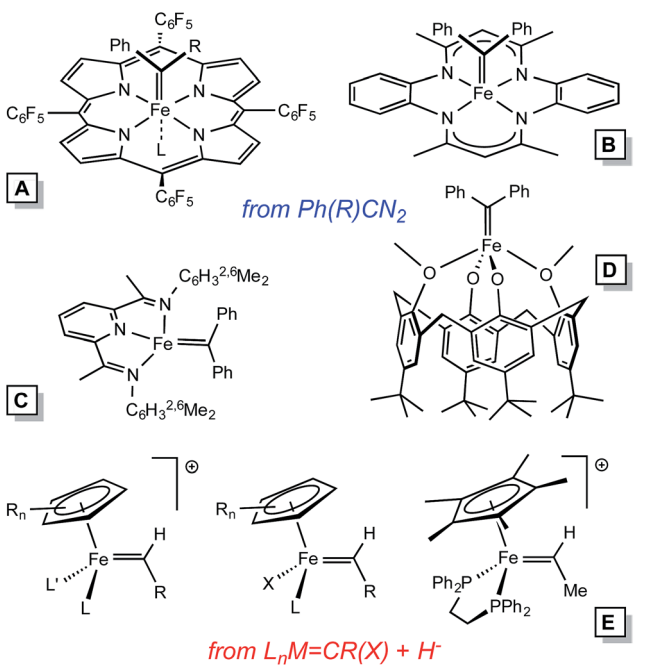

Fig. 1 Some iron alkylidenes and methods of synthesis.

[a]Department of Chemistry & Chemical Biology, Baker Laboratory, Cornell University, Ithaca, NY, 14850, USA. E-mail: ptw2@cornell.edu; Fax: +1 607 255 4137; Tel: +1 607 255 7220

[b]Department of Chemistry & Pharmacy, Friedrich Alexander University Erlangen-Nürnberg (FAU), Egerlandstr. 1, D-91058 Erlangen, Germany

† Electronic supplementary information (ESI) available. CCDC 1057828–1057831. For ESI and crystallographic data in CIF or other electronic format see DOI: 10.1039/c5sc01268f

implemented *via* precedented C–H bond activations by Karsch's *cis*-$Me_2Fe(PMe_3)_4$ (ref. 19) complex.[20–23] While viable olefin metathesis catalysts containing Fe have not yet been realized, the generality of this approach suggests that incremental advances may yet prove successful.

Results and discussion

Di-1,2-(*E*-2-(pyridin-2-yl)vinyl)benzene: tetradentate ligand precursor

As Scheme 1 illustrates, incorporation of two vinyl groups into a tetradentate chelate precursor was predicated on successful implementation of a Horner–Wadsworth–Emmons reaction to achieve the requisite *E*-stereochemistry. The modified 2-pyridinyl-methyl reagent was prepared according to a literature procedure[24] from $Na[OP(OEt)_2]$ and 2-pyridyl-methylchloride in 70% yield. Its addition to 1,2-benzene-dialdehyde afforded di-1,2-(*E*-2-(pyridin-2-yl)vinyl)benzene ($(bdvp)H_2$, $E/Z > 19:1$) in 37% yield upon crystallization from ether/hexane.

Tridentate ligand precursors: $PhCHNCH_2$(*E*-CH=CHPh) and PhCH=N(2-CCMe-Ph)

Condensation routes afforded the two additional tridentate ligands used in this study, as shown in Scheme 2. Cinnamyl amine[25] and benzaldehyde were used to synthesize $PhCH{=}NCH_2$(*E*-CH=CHPh) ($(pipp)H_2$),[26] while 2-propynyl-aniline, prepared from Pd-catalyzed cross-coupling[27] of propyne and 2-iodo-aniline, and benzaldehyde were used to generate PhCH=N(2-CCMe-Ph) ((pipa)H). A number of other potential imine and pyridine-containing tridentate ligand precursors were similarly made, but the subsequent C–H bond activations proved to be too slow or ineffective, allowing for competitive *cis*-$Me_2Fe(PMe_3)_4$ degradation.

Metalation *via* C–H bond activation and insertion

Treatment of *cis*-$Me_2Fe(PMe_3)_4$ (ref. 19) with the tetradentate precursor 1,2-(*E*-2-(pyridin-2-yl)vinyl)benzene ($(bdvp)H_2$) was undertaken at −20 °C in toluene. After 10 h, the solution was warmed to 23 °C and concentrated to afford $(bdvp)Fe(PMe_3)_2$ (**1**-PMe_3) in 84% yield as purple microcrystals (Scheme 3). The reaction is quite sensitive to steric bulk, as use of a precursor

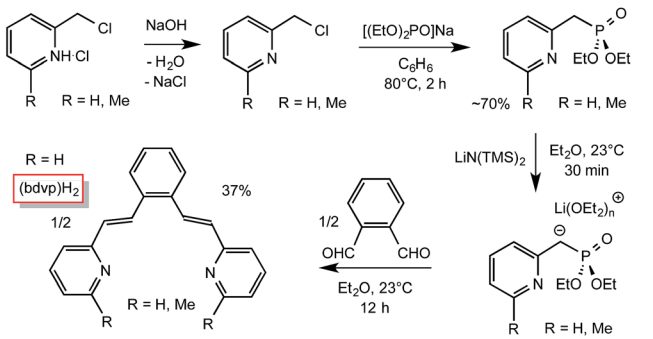

Scheme 1 Preparation of the divinyl ligand precursor, 1,2-(*E*-2-(pyridin-2-yl)vinyl)benzene ($(bdvp)H_2$).

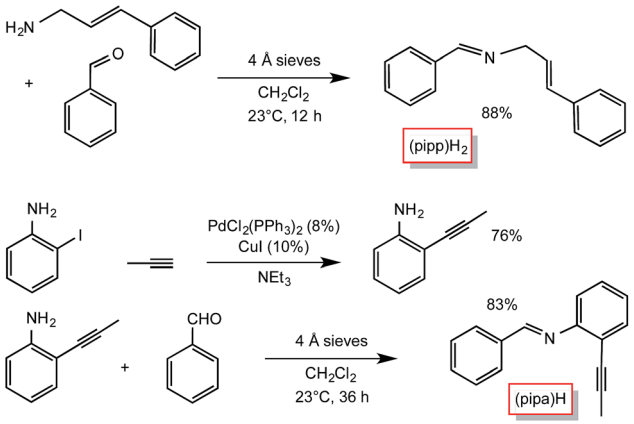

Scheme 2 Preparation of the tridentate precursors, $PhCH{=}NCH_2$(*E*-CH=CHPh) ($(pipp)H_2$) and PhCH=N(2-CCMe-Ph) ((pipa)H).

possessing *o*-Me groups on the pyridines (Scheme 1) failed to metalate, and decomposition of *cis*-$Me_2Fe(PMe_3)_4$ was instead observed.

A similar exposure of *cis*-$Me_2Fe(PMe_3)_4$ (ref. 19) to $PhCH{=}NCH_2$(*E*-CH=CHPh) ($(pipp)H_2$) in benzene at 23 °C after 20 h afforded a purple solid upon subsequent concentration (Scheme 3). Dissolution in THF under a dinitrogen atmosphere provided brown *trans*-$(pipp)Fe(PMe_3)_2N_2$ (**2**) in 63% yield after removal of solvent. It is likely that the *tris*-PMe_3 derivative is formed initially, but N_2 replaces PMe_3 in a probable dissociative process. Previous examples have shown that steric factors – in this case the phenyl substituent – labilize the phosphine opposite the imine.[23] The dinitrogen ligand is

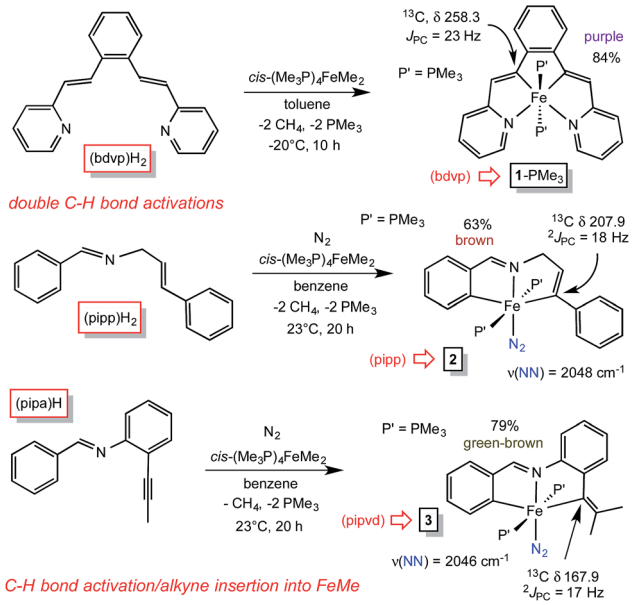

Scheme 3 Methods employed in synthesizing vinyl precursors derived from CH-bond activation/metalation of *cis*-$Me_2Fe(PMe_3)_4$ and acetylene insertion.

readily discerned *via* its IR spectrum, which reveals a ν(NN) at 2048 cm^{-1}.[28,29]

A third, different metalation was conducted with PhCH=N(2-CCMe-Ph) ((pipa)H) and *cis*-$Me_2Fe(PMe_3)_4$. The precedented imine-directed Ar-H activation occurred, followed by insertion of the pendant acetylene into the Fe–Me bond. The resulting complex, *trans*-(pipvd)$Fe(PMe_3)_2N_2$ (**3**), contains a dimethyl-vinyl group as the precursor to a potential alkylidene. Green-brown **3** was prepared in 79% yield after metalation for 20 h at 23 °C, and as in the previous case, it is likely an initially formed *tris*-PMe_3 complex lost a phosphine in the presence of N_2 to afford the dinitrogen complex,[23] whose ν(NN) is at 2046 cm^{-1}.

All three precursors feature downfield ^{13}C NMR chemical shifts for the vinyl carbons bound to iron. A triplet (J_{PC} = 23 Hz) corresponding to the Fe–C(Ar)= unit in (bdvp)$Fe(PMe_3)_2$ (**1**-PMe_3) was located at δ 258.3, an unusual shift that may be intrinsic to the metrics of its tetradentate chelation, *i.e.*, reflecting a very short *d*(Fe–C). The Fe–vinyl carbon of the tridentate chelate in *trans*-(pipp)$Fe(PMe_3)_2N_2$ (**2**) also manifests a significant downfield shift at δ 207.9 (t, J_{PC} = 18 Hz), while the Fe–C(Ar)= carbon of *trans*-(pipvd)$Fe(PMe_3)_2N_2$ (**3**), the most sterically hindered vinyl, resonates at δ 167.9 (t, J_{PC} = 17 Hz).

Structure of (bdvp)$Fe(PMe_3)_2$ (1-PMe_3)

Shown in Fig. 2 is the molecular structure of (bdvp)$Fe(PMe_3)_2$ (**1**-PMe_3), as determined by single crystal X-ray crystallography. The tetradentate ligand essentially resides in a plane of the pseudo-octahedral structure (∠C/N–Fe–P = 90.0(11)° (ave); ∠P1–Fe–P2 = 179.24(3)°), accompanied by *trans*-PMe_3 groups at *d*(Fe–P) = 2.2283(8) Å (ave). The *d*(Fe–N) of 2.060(4) (ave) are normal, but there is a splay in the N1–Fe–N2 angle (112.43(11)°) indicative of a strain in the chelate. The bite angles of the vinylpyridine are 81.01(13)° (ave), and the phenyl-divinyl bite angle is 85.61(14)°, hence the chelate angles sum to 360.1°.

Considerable distortion in the chelate is evident, as the iron–carbon bonds are quite short at 1.883(8) Å (ave), while the C6–C7–C8 and C13–C14–C15 angles of 127.4(4)° (ave) deviate significantly from 120°. Fig. 3 illustrates the chelate distances and angles in comparison to those of the related alkylidene complex (*vide infra*). All the angles about the Fe–C bonds are distorted in response to the proximity of the vinyl carbons to the iron. Note that the pyridines are not perfectly aligned as donors, as the Fe–N–C angles open to an average of 130.6(5)°.

Vinyl protonations lead to Fe(IV) alkylidenes

The vinyl precursors synthesized *via* the C–H bond activation and insertion processes were protonated[14–18] to yield cationic Fe(IV) alkylidenes, as illustrated in Scheme 4. The tetradentate chelate complex (bdvp)$Fe(PMe_3)_2$ (**1**-PMe_3) was treated with $H[BAr^F{}_4]$[30] in THF to afford orange [(bavp)$Fe(PMe_3)_2$][$BAr^F{}_4$] (**4**-PMe_3) in 80% yield. The lability of **1**-PMe_3 was tested with excess PMe_2Ph (10 equiv.), and repeated thermolyses in refluxing toluene, including periodic removal of PMe_3, were required to generate (bdvp)$Fe(PMe_2Ph)_2$ (**1**-PMe_2Ph). The dimethylphenylphosphine derivative **1**-PMe_2Ph was not isolated, and characterization using NMR spectroscopy proved elusive due to broadened and overlapping resonances. As a consequence, it was generated *in situ* and treated with $H[BAr^F{}_4]$ in THF to yield analytically pure [(bavp)$Fe(PMe_2Ph)_2$][$BAr^F{}_4$] (**4**-PMe_2Ph, 94%).

A related protonation of the tridentate chelate species *trans*-(pipp)$Fe(PMe_3)_2N_2$ (**2**) in THF initially gave a complex mixture that exhibited $^{31}P\{^1H\}$ NMR spectral resonances consistent with starting material, a tri-phosphine complex, and degradation products. The addition of PMe_3 to the reaction resulted in one major product, [(piap)$Fe(PMe_3)_3$][$BAr^F{}_4$] (**5**) that was isolated as yellow-orange microcrystals in 72% yield. It is likely that an initial dinitrogen-containing Fe(IV) product, [(piap)$Fe(PMe_3)_2N_2$]

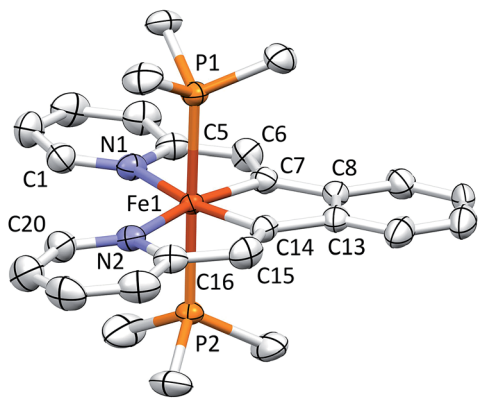

Fig. 2 Molecular view of (bdvp)$Fe(PMe_3)_2$ (**1**-PMe_3). Interatomic distances (Å) and angles (°): Fe–N1, 2.057(3); Fe–N2, 2.062(3); Fe–C7, 1.877(3); Fe–C14, 1.888(3); Fe–P1, 2.2285(8); Fe–P2, 2.2280(8); N1–Fe–C7, 81.10(13); N1–Fe–C14, 166.62(13); N1–Fe–N2, 112.43(11); N1–Fe–P1, 89.45(8); N1–Fe–P2, 91.17(8); C7–Fe–C14, 85.61(14); C7–Fe–N2, 166.35(13); C7–Fe–P1, 90.06(10); C7–Fe–P2, 89.61(10); C14–Fe–N2, 80.91(13); C14–Fe–P1, 89.03(9); C14–Fe–P2, 90.26(9); N2–Fe–P1, 91.84(8); N2–Fe–P2, 88.32(8); P1–Fe–P2, 179.24(3).

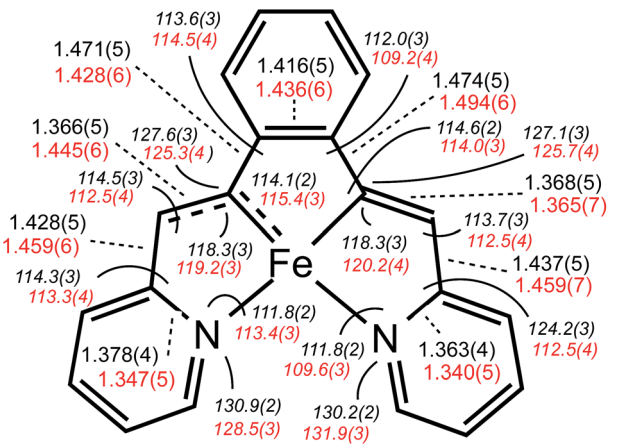

Fig. 3 Comparative ligand metric parameters (distances (Å), dashed black lines; angles (°, *italics*), curved black lines) for Fe(II) (bdvp)$Fe(PMe_3)_2$ (**1**-PMe_3, black) *vs.* Fe(IV) [(bavp)$Fe(PMe_3)_2$][$BAr^F{}_4$] (**4**-PMe_3, red).

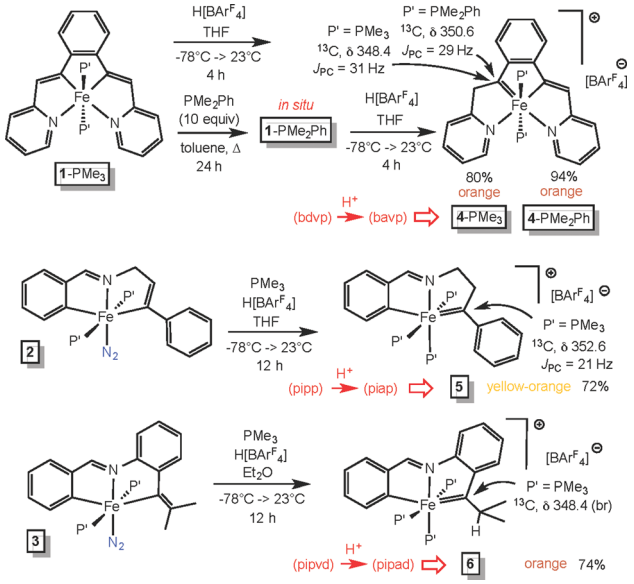

Scheme 4 Protonation with H[BAr$^F_4$] afforded cationic Fe(IV) alkylidenes.

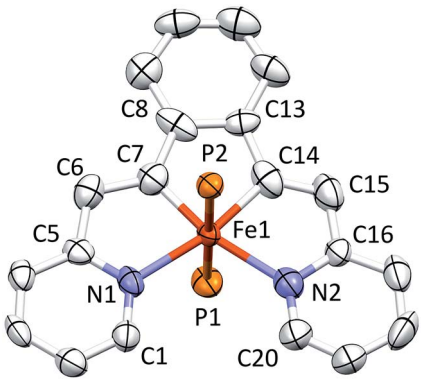

Fig. 4 Molecular view of the cation pertaining to [(bavp)Fe(PMe$_3$)$_2$][BAr$^F_4$] (**4**-PMe$_3$); the PMe$_3$ methyl groups have been removed for clarity. Interatomic distances (Å) and angles (°): Fe–N1, 2.083(3); Fe–N2, 2.129(4); Fe–C7, 1.809(4); Fe–C14, 1.858(4); Fe–P1, 2.2671(11); Fe–P2, 2.2725(11); N1–Fe–C7, 81.47(17); N1–Fe–C14, 168.31(19); N1–Fe–N2, 110.98(14); N1–Fe–P1, 88.53(9); N1–Fe–P2, 91.32(9); C7–Fe–C14, 86.9(2); N2–Fe–C7, 167.48(17); C7–Fe–P1, 91.87(13); C7–Fe–P2, 87.81(13); N2–Fe–C14, 80.71(18); C14–Fe–P1, 91.49(13); C14–Fe–P2, 88.60(13); N2–Fe–P1, 89.89(10); N2–Fe–P2, 90.44(10); P1–Fe–P2, 179.66(5).

[BAr$^F_4$], readily loses N_2, and through redistribution generates **5** along with decomposition products.

Protonation of (pipvd)Fe(PMe$_3$)$_2$N$_2$ (**3**) was conducted with H[BAr$^F_4$] in diethyl ether, and a mixture whose NMR spectra is related to that of the initial protonation of **2** was discerned. Again, the addition of PMe$_3$ to the reaction mixture permitted the isolation of [(pipvd)Fe(PMe$_3$)$_3$][BAr$^F_4$] (**6**) in 74% yield as orange microcrystals.

Definitive spectral characterization of the isolated Fe(IV) alkylidene complexes was predicated on observation of diagnostic downfield ^{13}C NMR resonances[31,32] attributed to the M=CRR′ functionality (Scheme 4). The spectral signatures were difficult to detect, requiring indirect methods, but the alkylidene chemical shifts for **4**-PMe$_3$, **4**-PMe$_2$Ph, **5**, and **6** were eventually observed at δ 348.4 (J_{PC} = 31 Hz), δ 350.6 (J_{PC} = 31 Hz), δ 352.6 (J_{PC} = 21 Hz), and δ 348.4 (br), respectively.

Structure of [(bavp)Fe(PMe$_3$)$_2$][BAr$^F_4$] (4-PMe$_3$)

A molecular view of the cation pertaining to [(bavp)Fe(PMe$_3$)$_2$][BAr$^F_4$] (**4**-PMe$_3$) is illustrated in Fig. 4, showing its distorted octahedral structure, with the tetradentate chelate occupying a single plane. The P–Fe–C/N angles average 90.0(15)°, and there is a splay in the bavp ligand indicated by the N1–Fe–N2 angle of 110.98(14)°, and the *trans*-N–Fe–C angles of 168.31(19) and 167.48(17)°.

The critical *d*(Fe=C7) is 1.809(4) Å, which is ~0.05 Å shorter than the adjacent iron–vinyl carbon distance of 1.858(4) Å. Both are shorter than the iron–carbon bond lengths in **1**-PMe$_3$, in contrast to the *d*(Fe–N), which are longer at 2.083(3) and 2.129(4) Å. As these changes and the comparison between **1**-PMe$_3$ and **4**-PMe$_3$ in Fig. 3 reveal, the chelate has pinched in to a slightly greater extent in the cation. The angles C6–C7–C8 and C13–C14–C15 are 2.3 and 1.4° less, respectively, than the corresponding angles in **1**-PMe$_3$, and the remaining chelate distances and angles change in concert.

Structure of [(piap)Fe(PMe$_3$)$_3$][BAr$^F_4$] (5)

Fig. 5 displays a molecular view of the cation corresponding to [(piap)Fe(PMe$_3$)$_3$][BAr$^F_4$] (**5**), and reveals its pseudo-octahedral geometry with the piap ligand occupying a *mer*-configuration about iron. The critical alkylidene distance, *d*(Fe–C10), is 1.867(7) Å, which is significantly shorter than *d*(Fe–C1) = 2.106(6) Å, but on par with the iron–vinyl carbon distances in **1**-PMe$_3$ (1.883(8) Å (ave)) and **4**-PMe$_3$ (1.858(4) Å). The tridentate chelate is strained, as the C1–Fe–C10 angle is 161.6(3)°, and the Fe–C10–C9 and Fe–C10–C11 angles of 115.7(5)° and 136.4(5)°, respectively, indicate that the alkylidene is not perfectly oriented. Note that the C10–Fe–P2 angles are 100.20(4)°; as a consequence, the d-orbital that comprises the iron portion of the Fe=C π-bond has some Fe–P σ* character that aids in producing better overlap with the carbon p-orbital.

Structure of [(pipad)Fe(PMe$_3$)$_3$][BAr$^F_4$] (6)

A molecular view of the cation of [(pipad)Fe(PMe$_3$)$_3$][BAr$^F_4$] (**6**) is provided in Fig. 6, which indicates the *mer*-octahedral structure of the iron alkylidene. The tridentate pipad chelate is essentially planar, and the isopropyl-aryl alkylidene possesses a *d*(Fe=C) of 1.899(3) Å, which is longer than the iron–vinyl carbon distances in **1**-PMe$_3$ and **4**-PMe$_3$. Again, the chelate exhibits strain about the core, as the C1–Fe–C17 angle is 163.36(15)°, and its isopropyl group exerts a steric influence on the unique PMe$_3$, as the C1–Fe–P1 angle is 104.46(12)°. The Fe–C1–C5 and Fe–C1–C2 angles are 112.8(2)° and 131.0(3)°, respectively, showing that the alkylidene is at an imperfect orientation with respect to the iron.

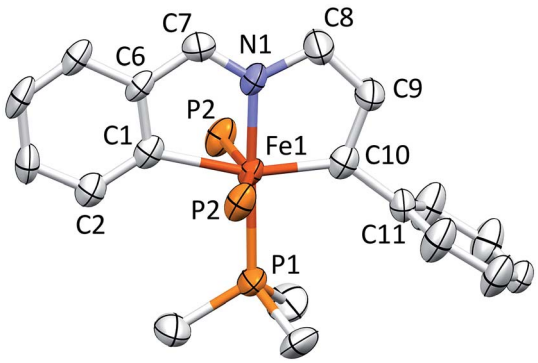

Fig. 5 Molecular view of the cation pertaining to [(piap)Fe(PMe_3)$_3$][$BAr^F{}_4$] (**5**); the methyl groups of the *trans*-PMe_3 ligands have been removed for clarity. Interatomic distances (Å) and angles (°): Fe–C1, 2.106(6); Fe–N1, 1.949(6); Fe–C10, 1.867(7); Fe–P1, 2.281(2); Fe–P2, 2.2733(16); C7–N1, 1.307(9); C1–Fe–N1, 78.4(3); C1–Fe–C10, 161.6(3); C1–Fe–P1, 103.7(2); N1–Fe–C10, 83.2(3); N1–Fe–P1, 177.94(17); C10–Fe–P1, 94.8(2); C1–Fe–P2, 79.47(4); N1–Fe–P2, 88.54(5); C10–Fe–P2, 100.20(4); P1–Fe–P2, 91.83(5); P2–Fe–P2, 158.89(8); Fe–C1–C2, 133.8(5); Fe–C1–C6, 110.4(5); Fe–C10–C9, 115.7(5); Fe–C10–C11, 136.4(5).

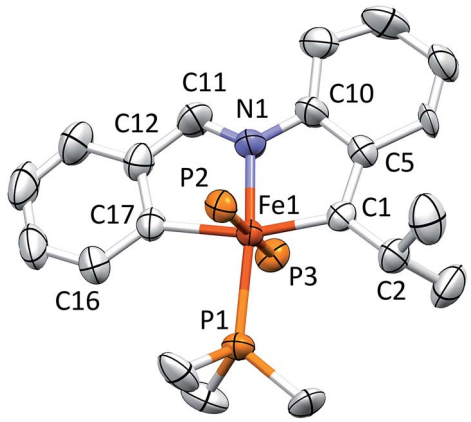

Fig. 6 Molecular view of the cation pertaining to [(pipad)Fe(PMe_3)$_3$][$BAr^F{}_4$] (**6**); the methyl groups of the *trans*-PMe_3 ligands have been removed for clarity. Interatomic distances (Å) and angles (°): Fe–C1, 1.899(3); Fe–N1, 1.933(3); Fe–C17, 2.059(3); Fe–P1, 2.317(2); Fe–P2, 2.226(3); Fe–P3, 2.367(3); N1–C11, 1.307(5); C1–C2, 1.525(5); N1–Fe–C17, 80.04(14); C1–Fe–C17, 163.36(15); C17–Fe–P1, 92.03(12); C17–Fe–P2, 88.28(13); C17–Fe–P3, 87.16(12); N1–Fe–C1, 83.34(14); N1–Fe–P1, 167.04(14); N1–Fe–P2, 96.52(16); N1–Fe–P3, 79.34(14); C1–Fe–P1, 104.46(12); C1–Fe–P2, 92.87(12); C1–Fe–P3, 90.53(13); P1–Fe–P2, 93.45(14); P1–Fe–P3, 90.11(13); P2–Fe–P3, 174.32(13); Fe–C17–C16, 136.0(3); Fe–C17–C12, 110.8(3); Fe–C1–C5, 112.8(2); Fe–C1–C2, 131.0(3).

Structural comparisons

In Table 1, a comparison of known Fe(IV) alkylidenes is given with reference to *d*(Fe=C) and ^{13}C NMR chemical shift (*δ*).[29,30] Paramagnetic derivatives are on the long side of the bond distance values, and the electronic structure analysis by Chirik *et al.*[13] of the PDI derivatives suggests that these species are best considered carbene radicals.[33] The π-interaction is construed as a carbene radical antiferromagnetically (AF) coupled to a metal dπ-electron of appropriate symmetry. Modern calculations have not been employed on Floriani's calix[4]arane diphenycarbene complexes,[11] but they are high spin, and therefore are likely to conform to an AF coupling model.

Of the remaining diamagnetic complexes, some relative distances appear to be a clear consequence of the *trans*-influence. When no ligand is opposite the diphenylcarbene, the distance is short, as in the cases of (tmtaa)Fe=CPh_2 (**B**)[10] and (TPFPP)Fe=CPh_2 (**A**).[12] As the methylimidazole adduct of the latter (*i.e.*, (TPFPP)Fe(=CPh_2)(MeIm) (**A**))[12] indicates, the distance is increased by 0.55 Å. It is not surprising that the complexes herein have *d*(Fe=C) that range from 1.809–1.899 Å, given the presence of a strong *trans*-influence ligand (an aryl). There is no straightforward correlation of *d*(Fe=C) to its respective ^{13}C NMR spectroscopic shift.

Mössbauer analysis of Fe(II) and Fe(IV) chelates

Shown in Fig. 7 are Mössbauer spectra of the related Fe(II) and Fe(IV) complexes *trans*-(pipvd)Fe(PMe_3)$_2$$N_2$ (**3**) and [(pipad)Fe(PMe_3)$_3$][$BAr^F{}_4$] (**6**), respectively. In Table 2, all Mössbauer parameters for the corresponding Fe(II) and Fe(IV) compounds are listed. The data in Table 2 reveal isomer shifts for the diamagnetic species all within Δ*δ* of 0.1 mm s^{-1}, and provide a textbook example of why they should not be simply correlated with formal oxidation state, but are strong indicators of covalency.[34,35] "Iron–ligand bond lengths play a decisive role for the isomer shift of a compound",[35] and the data in Table 2 and Fig. 2–4 bear this out. Minimal bond distance changes occur in the protonation of (bdvp)Fe(PMe_3)$_2$ (**1**-PMe_3) to afford [(bavp)Fe(PMe_3)$_2$][$BAr^F{}_4$] (**4**-PMe_3), and similarly small *d*(Fe-L/X) changes are likely in the related protonations, leading to small isomer shift differences.

One counter argument regarding interpretation of isomer shifts pertains to the somewhat arbitrary formalism of treating a Schrock alkylidene as a (2−) ligand, whereas a Fischer carbene, in which conjugated lone pairs can donate to the carbon

Table 1 Comparison of iron-alkylidene *d*(Fe=C) and ^{13}C NMR shift (*δ*)

Compound[a]	*d*(Fe=C) (Å)	*δ* (^{13}C=Fe)
(tmtaa)Fe=CPh_2 (**B**)[b]	1.794(3)	313.2
(TPFPP)Fe=CPh_2 (**A**)[c]	1.767(3)	359.0
[Cp*(dppe)Fe=CH(Me)]PF_6 (**E**)[d]	1.787(8)	336.6
[(bavp)Fe(PMe_3)$_2$][$BAr^F{}_4$] (**4**-PMe_3)	1.809(4)	350.6
(TPFPP)Fe(=CPh_2)(MeIm) (**A**)[c]	1.827(5)	385.4
[(piap)Fe(PMe_3)$_3$][$BAr^F{}_4$] (**5**)	1.867(7)	352.6
[(pipad)Fe(PMe_3)$_3$][$BAr^F{}_4$] (**6**)	1.899(3)	348.4
(^{Et}PDI)Fe=CPh_2 (**C**)[e]	1.9205(19)	*Para*
(^{Me}EtPDI)Fe=CPh_2 (**C**)[e]	1.9234(18)	*Para*
	1.9357(18)	*Para*
[*p*-^{t}Bu-calix[4](O)$_2$(OMe)$_2$]Fe=CPh_2 (**D**)[f]	1.943(8)	*Para*
[*p*-^{t}Bu-calix[4](O)$_2$(OSiMe$_3$)$_2$]Fe=CPh_2 (**D**)[f]	1.958(5)	*Para*
	1.973(5)	*Para*

[a] See Fig. 1 for ligand structural types corresponding to A–D. [b] Ref. 10. [c] Ref. 12. [d] Ref. 9. [e] Ref. 13. [f] Ref. 11.

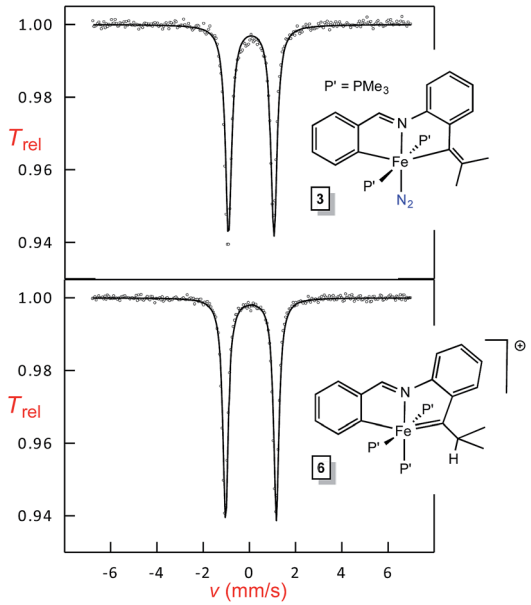

Fig. 7 Mössbauer spectra of Fe(II) *trans*-(pipvd)Fe(PMe_3)$_2N_2$ (**3**, $\delta = 0.07(1)$ mm s^{-1}; $\Delta E_Q = 1.97(1)$ mm s^{-1}), and the corresponding Fe(IV) cation [(pipad)Fe(PMe_3)$_3$][BAr^F_4] (**6**, $\delta = 0.07(1)$ mm s^{-1}; $\Delta E_Q = 2.20(1)$ mm s^{-1}).

(*i.e.*, M=CX(R) ↔ $M^{(-)}$–C=$X^{(+)}$ (R)), is neutral. While one can argue there is some conjugation for **3** and **6**, the other cases are less readily interpreted in this fashion, especially given the orientation of the phenyl group of **5** as roughly orthogonal to the Fe=C interaction. There can be little question that two pairs of electrons – one sigma and one pi – exist between iron and carbon in these compounds, and that the parameters of the Mössbauer spectra correlate with a strong degree of covalency. Previously characterized alkylidene species are limited to those reported by Chirik *et al.*,[13] whose $S = 1$ systems are sufficiently different to be essentially incomparable.

Interpretation of the quadrupole splitting (ΔE_Q), a measure of the electric field gradient at the nucleus,[35] is less transparent. The changes in ligand coordination, principally PMe_3 for N_2 in the conversion of **2** and **3** to **5** and **6**, respectively, are apparently significant enough to offset changes to the Ar-Fe(–Vy/=C) axes. For **1**-PMe_3 and **4**-PMe_3, there is a consequential change from $\Delta E_Q = 1.96(1)$ mm s^{-1} to 2.67(1) mm s^{-1}, as the rhombicity of the complex is notably altered due to the change from a symmetric divinyl coordination to that of the alkylidene and vinyl arrangement.

Conclusions

Protonation of Fe(II) chelate complexes in which iron–vinyl bonds are present led to the formation of four cationic Fe(IV) alkylidene complexes, three of which are structurally characterized. Prior to this study, [Cp*(dppe)Fe=CH(Me)]PF_6 was the only non-aryl Fe(IV) alkylidene that had undergone X-ray diffraction structural analysis, although numerous related [CpLL′Fe=CHR]$^+$ complexes have been synthesized.[7–9,14–16]

This study confers confidence in iron–vinyl protonation as a viable, general route to Fe(IV) alkylidenes in non-Cp systems. The compounds herein (*i.e.*, **4**-PMe_3, **5** and **6**) were not active towards metathesis (*e.g. cis*-2-pentene and RCCR; R = Me, Ph) or cycloprotonation, primarily because PMe_3 is not sufficiently labile, as expected. In order to implement this route toward viable olefin metathesis catalysts, future syntheses must address three factors: (1) complexes must be coordinatively unsaturated, with 14e$^-$ species the obvious targets based on ruthenium analogues; (2) complexes must be neutral or anionic, where the d-orbitals are less contracted; and (3) Fe=CHR moieties must be targeted.

Experimental section

Experimental details, full spectral characterizations, and a description of the Mössbauer spectroscopic analysis are given in the ESI.† For general descriptions, consult the schemes. Some crystallographic information is given below.

Crystal data for 1-PMe_3

$C_{26}H_{32}N_2P_2Fe$, $M = 490.33$, triclinic, $P\bar{1}$, $a = 10.2138(8)$, $b = 10.6014(8)$, $c = 12.4208(10)$ Å, $\alpha = 88.674(4)°$ $\beta = 67.062(3)°$, $\gamma = 89.687(4)°$, $V = 1238.24(17)$ Å^3, $T = 203(2)$ K, $\lambda = 0.71073$ Å, $Z = 2$, $R_{int} = 0.0311$, 22 420 reflections, 6098 independent, R_1(all data) = 0.0663, w$R_2 = 0.1766$, GOF = 1.077.†

Table 2 Comparison of Fe(II) and Fe(IV) alkylidene Mössbauer parameters

Compound	δ (mm s^{-1})	ΔE_Q (mm s^{-1})	Γ_{FWHM} (mm s^{-1})
(bdvp)Fe(PMe_3)$_2$ (**1**-PMe_3)	0.09(1)	1.96(1)	0.45(1)
trans-(pipp)Fe(PMe_3)$_2N_2$ (**2**)[a]	0.08(1)	2.14(1)	0.31(1)
trans-(pipvd)Fe(PMe_3)$_2N_2$ (**3**)	0.07(1)	1.97(1)	0.33(1)
[(bavp)Fe(PMe_3)$_2$][BAr^F_4] (**4**-PMe_3)[b]	0.01(1)	2.67(1)	0.28(1)
[(piap)Fe(PMe_3)$_3$][BAr^F_4] (**5**)[c]	0.06(1)	2.02(1)	0.29(1)
[(pipad)Fe(PMe_3)$_3$][BAr^F_4] (**6**)	0.07(1)	2.20(1)	0.28(1)

[a] Sample contained 20% of a high spin Fe(II) species: $\delta = 1.23(1)$ mm s^{-1}, $\Delta E_Q = 2.40(1)$ mm s^{-1}, $\Gamma_{FWHM} = 0.73(1)$ mm s^{-1}. [b] Sample contained 18% of a high spin Fe(II) species: $\delta = 1.28(1)$ mm s^{-1}, $\Delta E_Q = 2.70(1)$ mm s^{-1}, $\Gamma_{FWHM} = 0.54(1)$ mm s^{-1}. [c] Sample contained 35% of a high spin Fe(II) species: $\delta = 1.25(1)$ mm s^{-1}, $\Delta E_Q = 2.42(1)$ mm s^{-1}, $\Gamma_{FWHM} = 0.51(1)$ mm s^{-1}.

Crystal data for 4-PMe_3

$C_{58}H_{45}N_2F_{24}BP_2Fe$, M = 1354.56, monoclinic, $P2_1/c$, a = 19.6517(7), b = 12.5655(4), c = 25.3645(7) Å, β = 109.7450(10)°, V = 5895.1(3) Å^3, T = 203(2) K, λ = 0.71073 Å, Z = 4, R_{int} = 0.0365, 49 817 reflections, 12 059 independent, R_1(all data) = 0.0958, wR_2 = 0.1782, GOF = 1.012.†

Crystal data for 5(THF)

$C_{61}H_{60}NOF_{24}BP_3Fe$, M = 1438.67, monoclinic, $C2/m$, a = 19.963(5), b = 17.492(6), c = 19.586(6) Å, β = 93.869(14)°, V = 6824(4) Å^3, T = 203(2) K, λ = 0.71073 Å, Z = 4, R_{int} = 0.0579, 21 278 reflections, 5076 independent, R_1(all data) = 0.0899, wR_2 = 0.1923, GOF = 1.155.†

Crystal data for 6

$C_{58}H_{55}NF_{24}BP_3Fe$, M = 1381.60, monoclinic, $P2_1/c$, a = 18.4232(6), b = 13.0618(4), c = 25.9802(8) Å, β = 99.5300(10)°, V = 6165.6(3) Å^3, T = 233(2) K, λ = 0.71073 Å, Z = 4, R_{int} = 0.0393, 35 706 reflections, 9178 independent, R_1(all data) = 0.0780, wR_2 = 0.1273, GOF = 1.050.†

Acknowledgements

Support from the National Science Foundation (CHE-1402149), Cornell University, and Friedrich Alexander University is gratefully acknowledged.

Notes and references

1 H. Jeong, J. M. John, R. R. Schrock and A. H. Hoveyda, *J. Am. Chem. Soc.*, 2015, **137**, 2239–2242.
2 (*a*) R. R. Schrock, *Angew. Chem., Int. Ed.*, 2006, **45**, 3748–3759; (*b*) R. R. Schrock and A. H. Hoveyda, *Angew. Chem., Int. Ed.*, 2003, **42**, 4592–4633.
3 V. M. Marx, A. H. Sullivan, M. Melaimi, S. C. Virgil, B. K. Keitz, D. S. Weinberger, G. Bertrand and R. H. Grubbs, *Angew. Chem., Int. Ed.*, 2015, **54**, 1919–1923.
4 R. H. Grubbs, *Angew. Chem., Int. Ed.*, 2006, **45**, 3760–3765.
5 Y. Chauvin, *Angew. Chem., Int. Ed.*, 2006, **45**, 3740–3747.
6 O. Eisenstein, R. Hoffmann and A. R. Rossi, *J. Am. Chem. Soc.*, 1981, **103**, 5582–5584.
7 (*a*) M. Brookhart, J. R. Tucker and G. R. Husk, *J. Am. Chem. Soc.*, 1983, **105**, 258–264; (*b*) M. Brookhart and J. R. Tucker, *J. Am. Chem. Soc.*, 1981, **103**, 979–981; (*c*) M. Brookhart, D. Timmers, J. R. Tucker, G. D. Williams, G. R. Husk, H. Brunner and B. Hammer, *J. Am. Chem. Soc.*, 1983, **105**, 6721–6723.
8 G. Poignant, S. Nlate, V. Guerchais, A. J. Edwards and P. R. Raithby, *Organometallics*, 1997, **16**, 124–132.
9 V. Mahias, S. Cron, L. Toupet and C. Lapinte, *Organometallics*, 1996, **15**, 5399–5408.
10 A. Klose, E. Solari, C. Floriani, N. Re, A. Chiesi-Villa and C. Rizzoli, *Chem. Commun.*, 1997, 2297–2298.
11 V. Esposito, E. Solari, C. Floriani, N. Re, C. Rizzoli and A. Chiesi-Villa, *Inorg. Chem.*, 2000, **39**, 2604–2613.
12 Y. Li, J.-S. Huang, Z.-Y. Zhou, C.-M. Che and X.-Z. You, *J. Am. Chem. Soc.*, 2002, **124**, 13185–13193.
13 S. K. Russell, J. M. Hoyt, S. C. Bart, C. Milsmann, S. C. E. Stieber, S. P. Semproni, S. DeBeer and P. J. Chirik, *Chem. Sci.*, 2014, **5**, 1168–1174.
14 (*a*) K. A. M. Kremer, G.-H. Kuo, E. J. O'Connor, P. Helquist and R. C. Kerber, *J. Am. Chem. Soc.*, 1982, **104**, 6119–6121; (*b*) G.-H. Kuo, P. Helquist and R. C. Kerber, *Organometallics*, 1984, **3**, 806–808.
15 T. Bodnar and A. R. Cutler, *J. Organomet. Chem.*, 1981, **213**, C31–C36.
16 (*a*) A. Davison and J. P. Selegue, *J. Am. Chem. Soc.*, 1978, **100**, 7763–7765; (*b*) R. D. Adams, A. Davison and J. P. Selegue, *J. Am. Chem. Soc.*, 1979, **101**, 7232–7238.
17 M. I. Bruce and A. G. Swincer, *Aust. J. Chem.*, 1980, **33**, 1471–1483.
18 C. P. Casey, W. H. Miles, H. Tukada and J. M. O'Connor, *J. Am. Chem. Soc.*, 1982, **104**, 3761–3762.
19 H. H. Karsch, *Chem. Ber.*, 1977, **110**, 2699–2711.
20 (*a*) G. Xu, H. Sun and X. Li, *Organometallics*, 2009, **28**, 6090–6095; (*b*) X. Xu, J. Jia, H. Sun, Y. Liu, W. Xu, Y. Shi, D. Zhang and X. Li, *Dalton Trans.*, 2013, 3417–3428.
21 (*a*) R. Beck, T. Zheng, H. Sun, X. Li, U. Flörke and H.-F. Klein, *J. Organomet. Chem.*, 2008, **693**, 3471–3478; (*b*) S. Camadanli, R. Beck, U. Flörke and H.-F. Klein, *Organometallics*, 2009, **28**, 2300–2310; (*c*) H.-F. Klein, S. Camadanli, R. Beck, D. Leukel and U. Flörke, *Angew. Chem., Int. Ed.*, 2005, **44**, 975–977; (*d*) H.-F. Klein, S. Camadanli, R. Beck and U. Flörke, *Chem. Commun.*, 2005, 381–382.
22 E. C. Volpe, P. T. Wolczanski and E. B. Lobkovsky, *Organometallics*, 2010, **29**, 364–377.
23 E. R. Bartholomew, E. C. Volpe, P. T. Wolczanski, E. B. Lobkovsky and T. R. Cundari, *J. Am. Chem. Soc.*, 2013, **135**, 3511–3527.
24 T. Yamamori, K. Nagata, N. Ishizuka and K. Hayashi, Utilities of Olefin Derivatives, US Patent Appl. No. 10/489, 365, 2004.
25 N. Rodrigues, K. Bennis, D. Vivier, V. Pereira, C. F. Chatelain, E. Chapuy, H. Deokar, J. Busserolles, F. Lesage, A. Eschalier and S. Ducki, *Eur. J. Med. Chem.*, 2014, **75**, 391–402.
26 G. Wolf and E.-U. Würthwein, *Chem. Ber.*, 1991, **124**, 655–663.
27 (*a*) C. Shi, Q. Zhang and K. K. Wang, *J. Org. Chem.*, 1999, **64**, 925–932; (*b*) H. Kusama, J. Takaya and N. Iwasawa, *J. Am. Chem. Soc.*, 2002, **124**, 11592–11593.
28 J. L. Crossland and D. R. Tyler, *Coord. Chem. Rev.*, 2010, **254**, 1883–1894.
29 N. Hazari, *Chem. Soc. Rev.*, 2010, **39**, 4044–4056.
30 M. Brookhart, B. Grant and A. F. Volpe Jr, *Organometallics*, 1992, **11**, 3920–3922.
31 J. Louie and R. H. Grubbs, *Organometallics*, 2002, **21**, 2153–2164.
32 J. Feldman and R. R. Schrock, in *Prog. Inorg. Chem.*, ed. S. J. Lippard, Wiley and Sons, New York, 1991, vol. 39, pp. 1–74.
33 W. I. Dzik, X. P. Zhang and B. de Bruin, *Inorg. Chem.*, 2011, **50**, 9896–9903.
34 F. Neese, *Inorg. Chim. Acta*, 2002, **337**, 181–192.
35 P. Gütlich, E. Bill and A. X. Trautwein, *Mössbauer Spectroscopy and Transition Metal Chemistry: Fundamentals and Applications*, Springer-Verlag, Berlin, 2011.

